EMI Noise Properties of the NICMOS Cooling System as Seen by a NICMOS-3 Flight Spare Detector (or, Turing NICMOS into a Spectrum Analyzer)

Glenn Schneider, NICMOS Project, University of Arizona
May 1, 1998

0. SUMMARY

Analysis of power spectra obtained from images taken with a NICMOS-3 flight spare detector and configured test dewar electrically connected to the NCS reveal low-level broad-band induced power in the images in the ~5kHz-9kHz region, along with a narrow-band power contributor at 4051 kHz. While the total power contributed by the NCS is very small compared to the overall systemic noise its non-random nature can generate image artifacts on small spatial scales which may not be insignificant. The non-NCS environmental noise was elevated significantly from what we would expect in flight (mainly due to the VEST/BRZ), and hence the magnitude of the NCS induced noise wrt the performance of the flight system will be proportionately greater. Because of the differences in instrumental configuration, and overall systemic noise in the EMI test environment, it is difficult to assess whether the total noise in these frequency bands will actually have any significant effect on NCS-era NICMOS science. This is discussed in more detail in the report that follows. There is, however, a discernible increase in noise, corresponding to an increase of ~9% in the systemic per read-pair intrinsic measurement error (i.e., array-averaged) read noise. This temporal characteristics of the NCS-induced noise, however, act over only ~ 6% of the sampling frequencies detectable by NICMOS, and hence may have consequences in terms of introducing low-level structural artifacts on ~10 pixel linear scales in NICMOS image data. This probably warrants some effort to identify and reduce this noise source.

1. INTRODUCTION

On April 27, 1998, as part of the NICMOS cryo-cooler testing program, NICMOS Project/UofA personnel (Schneider and Hubbard) conducted an experiment to ascertain the possible susceptibility of a NICMOS-3 detector to conducted and/or radiated electromagnetic interference from the cryo-cooler. A flight-spare detector on a flight mount in a UofA test dewar, was shipped to GSFC for this investigation. All control, signal, data, and power connections were made between the test dewar and a functional replica of the NICMOS flight electronics (a "Baseline Release Zero, or BRZ rack) in an electrically flight-like configuration. Grounding and mechanical connections to the test dewar and the cryo-cooler system were also established (by Creare and GSFC personnel) to emulate flight-like conditions. Testing was carried out in an EMI clean/screen room to attenuate outside interference. A series of images were obtained to map the spectral frequencies of any NCS induced EMI in NICMOS science data. Data were obtained using in-flight detector timing and clocking patterns as per normal on-orbit operations via stored command loads executing on a SITS system.

2. SAMPLING STRATEGY USING NICMOS-3 DETECTOR AND FSW 4.0A

The NICMOS-3 detectors are 256x256 pixel MgCdTe photodiode arrays, indium-bump bonded to a sapphire substrate and employing a silicon multiplexor. The array is "divided" into four quadrants with separate read-out amplifiers, down-stream A-to-D converters and associated electronics. The instantaneous charge on a pixel may be read non-destructively, permitting multiple samples to measure charge accumulation over time. Pixels in each quad are accessed sequentially with a 10.5 micro-second horizontal pixel clock. At the end of a horizontal line incrementation of the vertical line clock requires two cycle-times of the horizontal clock (i.e., the horizontal timing is "overclocked" by 21 microseconds at the end of a row). Thus, the time required to read out all pixels in a quadrant is 174.7 milliseconds. Pixels with identical horizontal and vertical offsets from the base addresses of each of the 4 quads are accessed and read out simultaneously.

The data acquisition mode for this test employed the standard "fast" (i.e., non-parallel) Multiple Accumulate (multiaccum) detector timing pattern and flight S/W. The initialization of this mode incorporates a triple global reset of all pixels in each quad (sequentially by pixel). Following this the output amplifiers are enabled (they are normally kept off during integrations, except when reading out, to minimize amplifier glow) as the [row,column] address of the pixel clock is set to [0,0]. Pixels are clocked immediately. Because some time is required for both the amplifier to stabilize, and for an exponential post-reset signal gradient (the "shading") to decay, 20 rows of pixels are clocked over 27.3 milliseconds. The address pointer is then reset to the [0,0] pixel in each quad and the initial post-reset data readout to be collected begins 202 milliseconds after that pixel is reset. Since all pixels are read sequentially within a quad over 174.7ms any periodically induced signals can be seen with frequencies between 5hz and 50,000hz in a single read. Since all 4 quads are read simultaneously through different read-out electronics, four independent measurements of such impressed signals are obtained. Power spectra derived from each of the 4 quads may be combined to improve delectability with a S/N increase of 2.

The initial read through the array determines the DC level of each pixel 202ms after each pixel is reset. The array can then be re-read as charge accumulates up to 25 additional times, with time-variable (selectable) wait intervals between subsequent readouts. For this test, equally spaced wait interval were selected to obtain a1.2 second spacing between subsequent readouts. This pattern of 26 reads of the array, spaced by 1.2 seconds, was repeated three times with 10 seconds between the start of each multiaccum integration. In principle, this sampling pattern allows looking at frequency components in the sub 5Hz domain, though this has not been done at the time of this report. Multiple repeats of the blocks of three 26-read multiaccums were executed to obtain higher S/N in the measurements to allow greater sensitivity in signal detecdtion, and to verify repeatability and stability of the measurements and to look for longer timescale secular/temporal variability.

3. DIFFERENCES FROM FLIGHT

The flight spare detector was cooled and stabilized to LN2 temperature (~77K) in the test dewar before any measurements were taken. This is ~16K warmer then the current in-flight operating temperature of the NICMOS detectors, and ~3-5K warmer then the anticipated operating temperature of the detectors when cooled with the NCS. Dark currents at 77K are approximately 1e-/second, slightly higher, but comparable to what is expected in flight with the NCS. This is about an order of magnitude higher then the dark currents currently seen with the NICMOS solid-N2 cryostat.

The output voltage of the detector changes as a function of temperature. In order to stay within the dynamic range of the A-to-D converters the DC offset voltage must be adjusted. For this test, such an adjustment was made after the BRZ and detector were brought up to an operate state. The adjustment was made empirically to bring the no-signal output level to near mid-scale in the conversion range. (Actually, ~5800 ADU in the range of +/-32,767K ADU). Thus, the dark image frames have much higher count values then one is used to seeing from flight data, but this is not relevant to this test.

In this report, a conversion gain of 5.4e- /ADU is assumed from previous calibration of this detector operated in a manner consistent with the voltage inputs supplied by the BRZ. No special re-calibration was done as part of this test to re-determine the conversion gain.

4. SEPARATING OUT NON-CRYO COOLER SIGNALS

Detected signals and image artifacts due to the intrinsic properties of the flight-spare detector and the BRZ electronics had to be identified to separate these from any cryo-cooler induced signatures seen in the images. Several such artifacts were found and should be understood if others will look at these data in the future. In general the BRZ unit used for this test was obtained from the VEST (building 29) and is much noisier then the BRZ unit in the ESTF lab (building 314) which was used in previous non-related testing with our flight-spare array and test dewar. Much effort was expended by Ball and UofA to reduce the noise levels in the ESTF/BRZ last year (which also had noise problems) to support testing of the development of a new auto-flush detector timing pattern. If additional H/W testing is to be done with a NICMOS detector either the ESTF/BRZ should be used, or some effort should be made to reduce the noise in VEST/BRZ. Ultimately, the noise induced by the VEST/BRZ was the limiting factor in our detection sensitivity and complicated the analysis of the test data.

A) BRZ/ Low Voltage Power Supply (LVPS) synchronization with detector horizontal clock. Pre-flight, it was originally intended to run the NICMOS detectors with a 12.5 microsecond horizontal line clock. Testing with the flight electronics found very significant levels pattern noise induced by the DC-switching NICMOS low voltage power supply. The intrinsic noise problem, per se, in the supply as never fixed (eg., the switching frequency of the supply is not phase-locked to the pixel clock). However, an operational "fix" was adopted. The base rate for the horizontal pixel clock was changed to 10.5 microseconds, and quantized "wait states" in the downloadable timing patterns (the integration times) were enforced by ground-operations such that only an integral number of 250-nanosecond wait-state quanta of the timing-pattern generator were permitted to achieve synchronization with the LVPS. This works well in flight, and in the ESTF/BRZ, but apparently not with the VEST/BRZ as the characteristic vertical line (column) striping associated with this noise source appeared.

Had time permitted we may have found an empirical phase-delay in the timing pattern generator to reduce this, but the test timeline did not permit such an investigation. To ascertain the magnitude of this noise source which appears in individual reads, 3-sigma clipped column-means were taken to establish a representative level of a column (to average out pixel-to-pixel and read-noise variations). Since there is large scale structure over hundreds of ADUs across the array in the DC zero level, a third order polynomial fit was made to column-averages to remove the global array structure. The statistics of the "odd" and "even" column-means were then computed to ascertain the magnitude of the LVPS/pixel clock asynchronization noise.

This was done for 60 image frames (which were 30 multiaccum 2-read pairs taken to assess the read noise). The magnitude of the column noise was found to be ~56ADU (~300 electrons). This is extremely high. In flight the RMS read noise is an order of magnitude less then this. However, this noise is extremely repeatable, with a period of 21 microseconds, and subtracts out either in multi-accum first-difference pairs, or when subtracting a same-read from a reference dark. The latter was ultimately used to determine the intrinsic noise induced by the cryo-cooler.

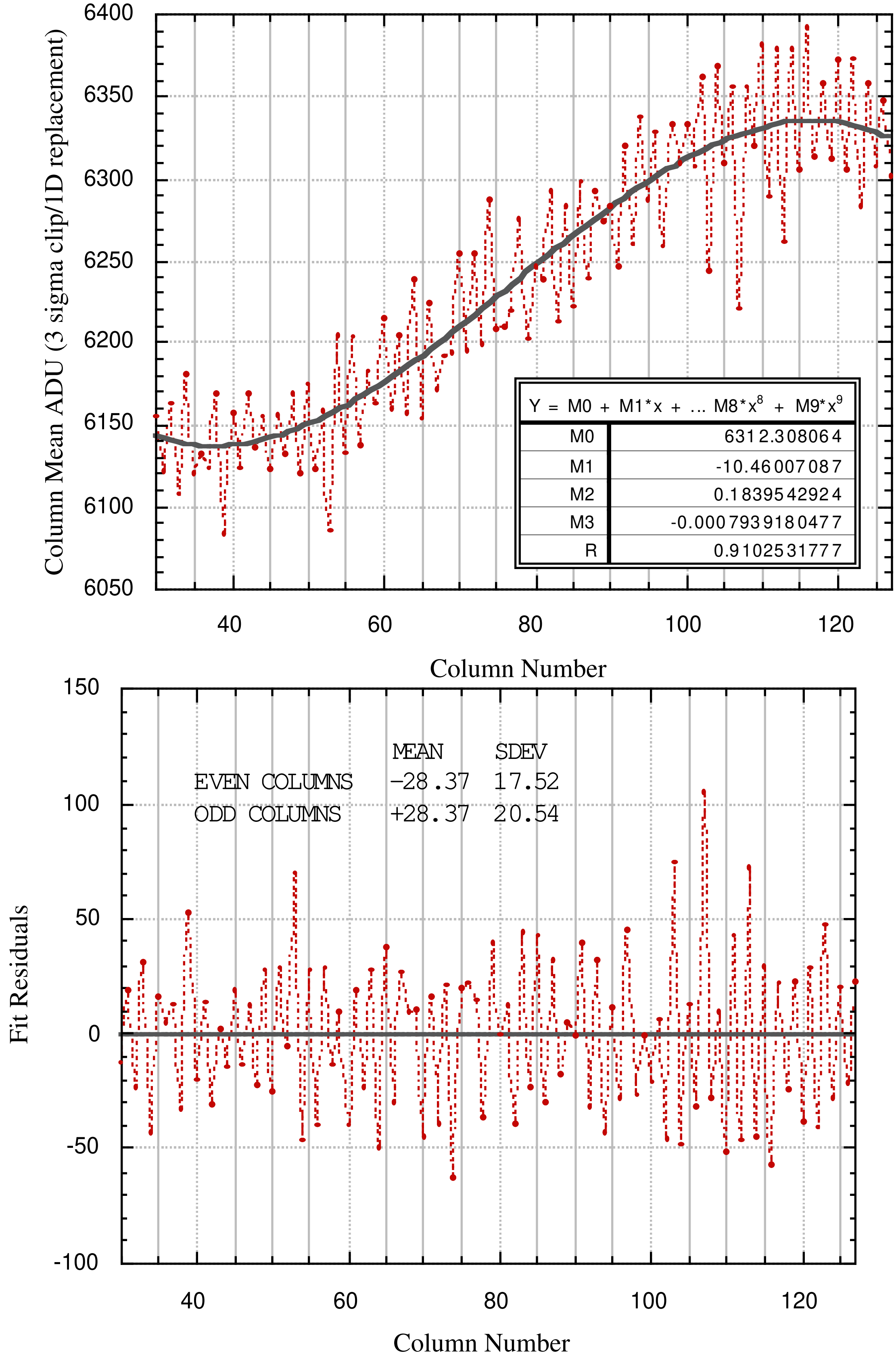

Figure 1. LVPS induced "column" noise.

B) BRZ induced and/or environmental 60Hz noise. There is a strong power peak at 60 Hz in all of the derived power spectra obtained with the flight spare detector. We see this in the power spectra whether the NCS was on or off. This does not perfectly subtract out in calibration (though it could in post-process Fourier filtering). We do not see this, significantly, in images taken with the inputs to the buffer box shorted (with the detector removed to measure the intrinsic noise of the BRZ/NICMOS electronics). This 60 Hz component then is very likely environmental, not NCS, though this should be independently considered and verified. See Figure 2.

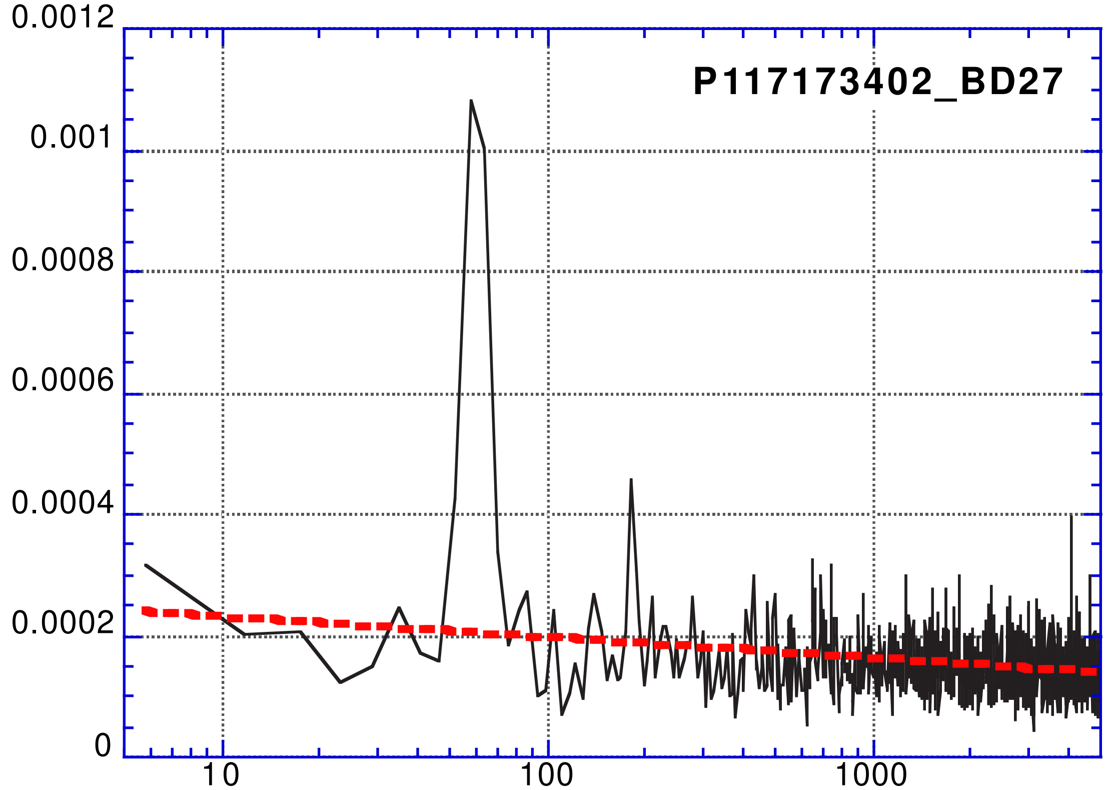

Figure 2. Representative 60Hz Noise in NCS OFF 5Hz - 5Khz Power Spectrum

C) Read Noise with the BRZ. Calibration data were obtained to assess the systemic noise characteristics (i.e., broadening of the intrinsic detector read noise by additional noise in or induced by the BRZ electronics). The composite read+electronic noise was ascertained by looking at differenced 2-read pairs with very short integration times and looking at the statistics of the difference frames. The mean of the standard deviations of the pair differences over all pixels for the 30 paired frames was 11.55ADU. For a single read-pair the noise would increase by root(30). This gives an extremely high estimate of the systemic 1-sigma electronic+read noise of 63ADU, or 341 electrons. This is an order of magnitude higher then the intrinsic read noise of the device which is known to be ~ 35e- per read pair. This implies that the BRZ electronics was contributing to or inducing an additional ~310e- of noise over and above the detector read noise.

To separate the noise induced by BRZ rack into the detector, from that induced into the down-stream replica electronics (housed in the BRZ rack), the buffer box inputs were shorted (i.e., taking the detector out of the loop). This provides a constant zero level into the NICMOS replica electronics. With NICMOS itself, and the ESTF/BRZ in such a configuration the measured 1-sigma dispersion in measured charge across all 64K measures per read is ~ 1ADU (due primarily to digital quantization in the A-to-D converters). With the VEST/BRZ this dispersion found to be 26.6 (+/-0.3) ADU, or ~ 144 electrons. The repeatability of this measure was tested by looking, as above, at the statistics of the differenced 2-pair reads, but with the shorted buffer box.. The mean of the standard deviations of the pair differences over all pixels for the 30 paired frames was 4.9 (+/-0.8) ADU. Again, this would increase by root(30) for a single read pair to 26.9 ADU, or 145 electrons. Thus, the same answer is obtained by looking at dispersion measure across the shorted input in single reads, or the statistics of read pairs. This indicates that roughly half (47%) of the total systemic elevated noise originates in the replica electronics, and half (53%) is induced into the detector.

This extremely high noise level was the primary contributor to the elevated BRZ-induced noise levels which persisted through the test. This noise, however, has a spectral 1/f characteristic, so it does not induce power peaks at particular frequencies. It did, however, lower our sensitivity so we could not detect low-level signals to a noise floor which could be seen on-orbit.

5. CALIBRATION OF NCS-ON IMAGES

To remove the non-NCS periodic noise sources, detector spatially-dependent DC offsets, and detector periodic noise (which would appear when the vertical line clock wraps, if the detector spatial-scale DC levels are not removed), a "reference dark" frame was made for each read. The "reference dark" data were taken with the NCS off from image sets timetageed from 98117.1534 to 98.1171612. The reference dark frame for each read was made by a medianing 18 multiaccums sampled in the same manner as the data taken with the NCS running. Root-N improvement in the noise was achieved, but the absolute level of the "read noise" in the dark calibration frames was very high due to the BRZ noise discussed above. This was checked by "self-calibration", that is subtracting the reference dark from each of the individual darks. The same levels of RMS "read noise" discussed in section 4.C was seen. This reference dark was subtracted from all of the NCS-On image data.

A set of post-test NCS-off darks were taken at the completion of the test. The original intention was to obtain a "pre" and "post" set of reference darks to be combined, or to permit interpolative dark subtraction if required. Near the end of the NCS-On testing the ground configuration was changed which resulted in subtle changes in the very low-level noise spectra. This configuration was in place when the post-test darks were taken. Because of the differences it was deemed prudent not to combine these data sets. That said, however, subtraction of the pre-test reference dark from individual post-test dark frames, have essentially the same read-noise distribution functions.

6. RAW AND REDUCED DATA

To measure the noise induced by the NCS, power spectra were computed for the reference dark subtracted individual NCS-On multiaccum reads. These were not power spectra of dark subtracted difference (rate) frames, but of the reads themselves. Because the 21 microsecond overclocking at the end of each horizontal row of pixels, discrete, rather than fast, Fourier transforms were used in obtaining the power spectra. As a result of a non-reproducibility in the absolute median DC level for a given read in different multiaccums, the DC levels of all pixels "float" a bit when subtracted from the reference dark. That is, the same read from different dark subtracted NCS-On multiaccums may have different per quadrant median levels. However, within the measurement error (read noise) this appears only as a constant offset. Since we are looking here for periodic noise this is not relevant.

The numerous power spectra obtained are too voluminous to produce in this report. The raw data (images reprocessed into FITS) files, and reduced power spectra (as ASCII files) will be available from an anonymous ftp site after May 2 for about a month at:

```
ftp starsrus.as.arizona.edu
cd CRYOEMI
```

After that time the data may be requested from the author as needed. The image files should be transferred as binary and the power spectra as ASCII.

The data files are subdivided into subdirectories timetagged by the time at which a set of images were "dumped" (i.e., transferred from the NICMOS/BRZ to the data acquisition machine). Thus, many data sets and power spectra have the same timetag. A subsequent observation identifier is used to sort out the time ordering of the individual files. The observation set number is a two digit base 36 number which increments monotonically for each section of the test (though it is repeated in some cases for different test sections). Within the observation set number a running counter is used for each readout which increments monotonically from 01 to 78 (26 reads per multi accum repeated insets of 3) for all but the initial check and read noise images.

The ASCII power spectra files give the frequency in column 1, and the corresponding power contributor measured in each of the four quads of the detector in columns 2-5, respectively. The first record of the file gives the DC power level, which is non-zero if the mean measured signal level across all pixel in the quad was not zero. A key to these data, by "dump" times is as follows:

```
         SYSTEM CHECK AND CALIBRATION
1171508  Initial Check Image
1171527  Read Noise (30 Images, 2-read pairs)

         PRE-TEST NCS-OFF DARK FRAMES
1171534  NCS OFF Group 1 of 26-read Multiaccums
1171541  NCS OFF Group 2 of 26-read Multiaccums
1171548  NCS OFF Group 3 of 26-read Multiaccums
1171600  NCS OFF Group 4 of 26-read Multiaccums
1171612  NCS OFF Group 5 of 26-read Multiaccums
1171619  NCS OFF Group 6 of 26-read Multiaccums

         NCS ON                                  SPEED
1171722  NCS ON  Group 1 of 26-read Multiaccums  4500Hz
1171734  NCS ON  Group 2 of 26-read Multiaccums  4800Hz ~WALL CLK
1171741  NCS ON  Group 3 of 26-read Multiaccums  5000Hz  13:35
1171748  NCS ON  Group 4 of 26-read Multiaccums  5000Hz  13:50
1171801  NCS ON  Group 5 of 26-read Multiaccums  5500Hz  13:52
1171811  NCS ON  Group 6 of 26-read Multiaccums  6000Hz  13:55
1171823  NCS ON  Group 7 of 26-read Multiaccums  *       14:19
1171830  NCS ON  Group 8 of 26-read Multiaccums

         POST-TEST NCS-OFF DARK FRAMES
1171922  NCS OFF Group 1 of 26-read Multiaccums
1171929  NCS OFF Group 2 of 26-read Multiaccums
1171936  NCS OFF Group 3 of 26-read Multiaccums

         SHORTED BUFFER BOX (GROUND FROM BOX TO BUILDING)
1172142  NCS OFF (30 Images, 2-read pairs)
1172149  NCS OFF Group 1 of 26-read Multiaccums
1172156  NCS OFF Group 2 of 26-read Multiaccums
1172203  NCS OFF Group 3 of 26-read Multiaccums
```

* Data, unfortunately, not transferred before UofA computer packed, to be recovered.

7. DISCUSSION

In the absence of any spectral signatures, uncorrelated random noise has a 1/f spectrum. The underlying power spectra with the NCS OFF, when one eliminates the other sources already discussed, is essentially 1/f (Fig 3, top). With the NCS ON, however, additional broadband power is seen in the images in the approximately 5kHz to 9kHz regime (Fig 5.3, bottom).

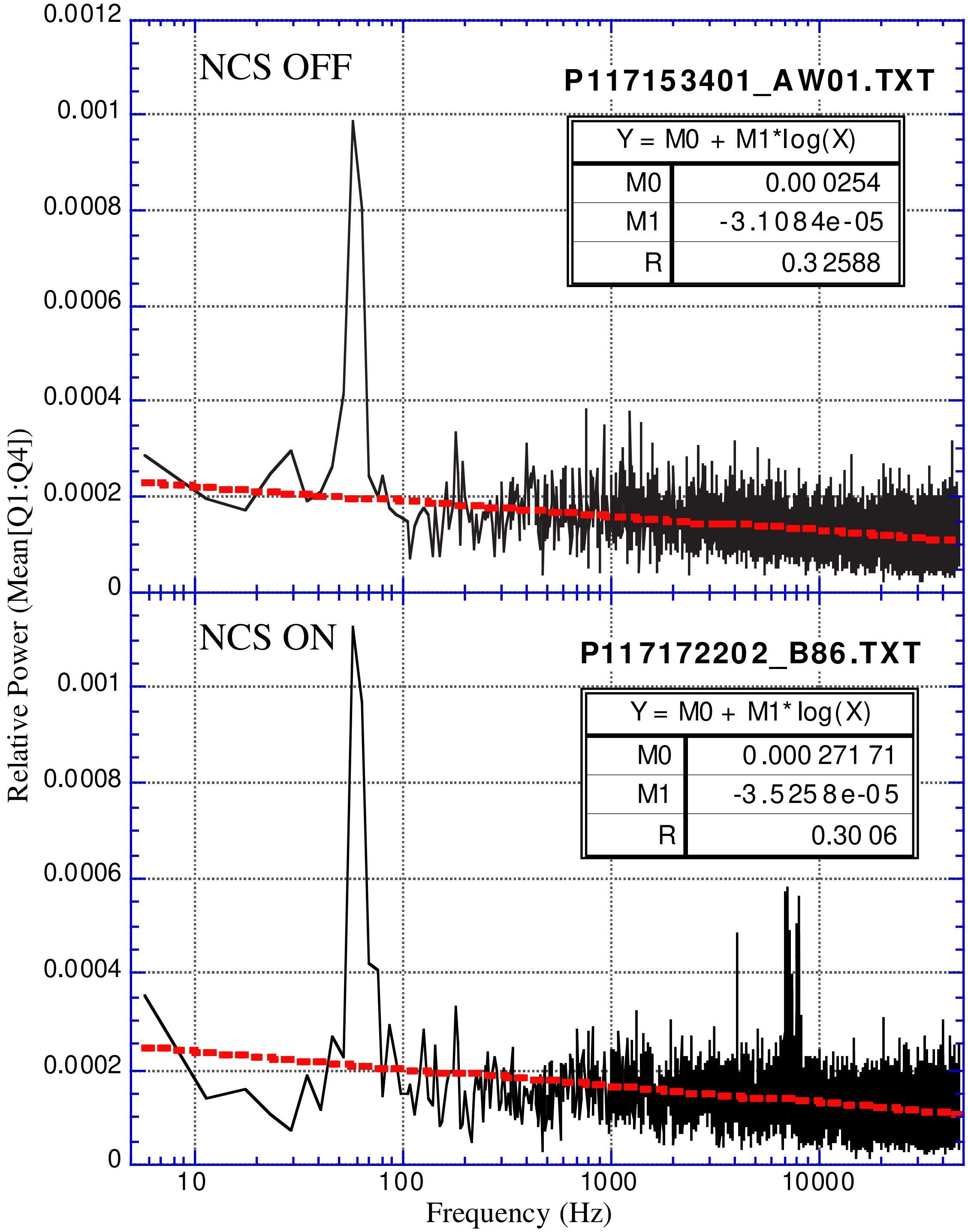

Figure 3. Representative NCS OFF and NCS ON Power Spectra

The 5kHz - 9kHz NCS induced power contributors appear to have a bi-modal frequency distribution, and indeed may originate from two different sources. A instantaneous detailed view of this spectral signature, for a single read (4 quad average) of the array is shown in Figure 4. The frequency spectrum of both components is time variable, but the integrated power is essentially constant and seem to shift downward in frequency with time (see figure 5). This may be correlated with the NCS turbine speed, which was initially ramping up during this period, though of course, it may be due to another secularly changing phenomenon. In addition, a sharp power spike is seen at 4051 Hz in the NCS ON spectra. The total power here is very small, but may be indicative of the source of the broader-band contributors.

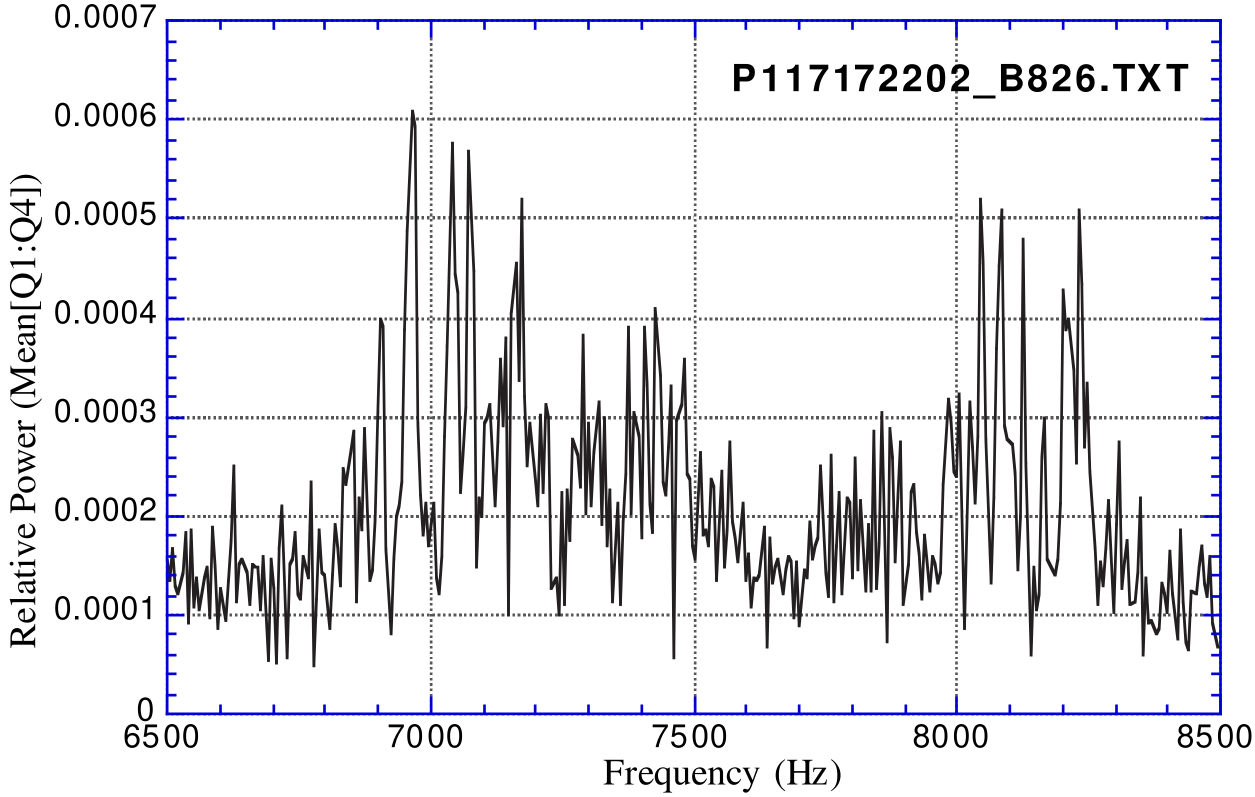

Figure 4. Representative Spectral Signature of NCS induced Power @ ~ 7.5kHz

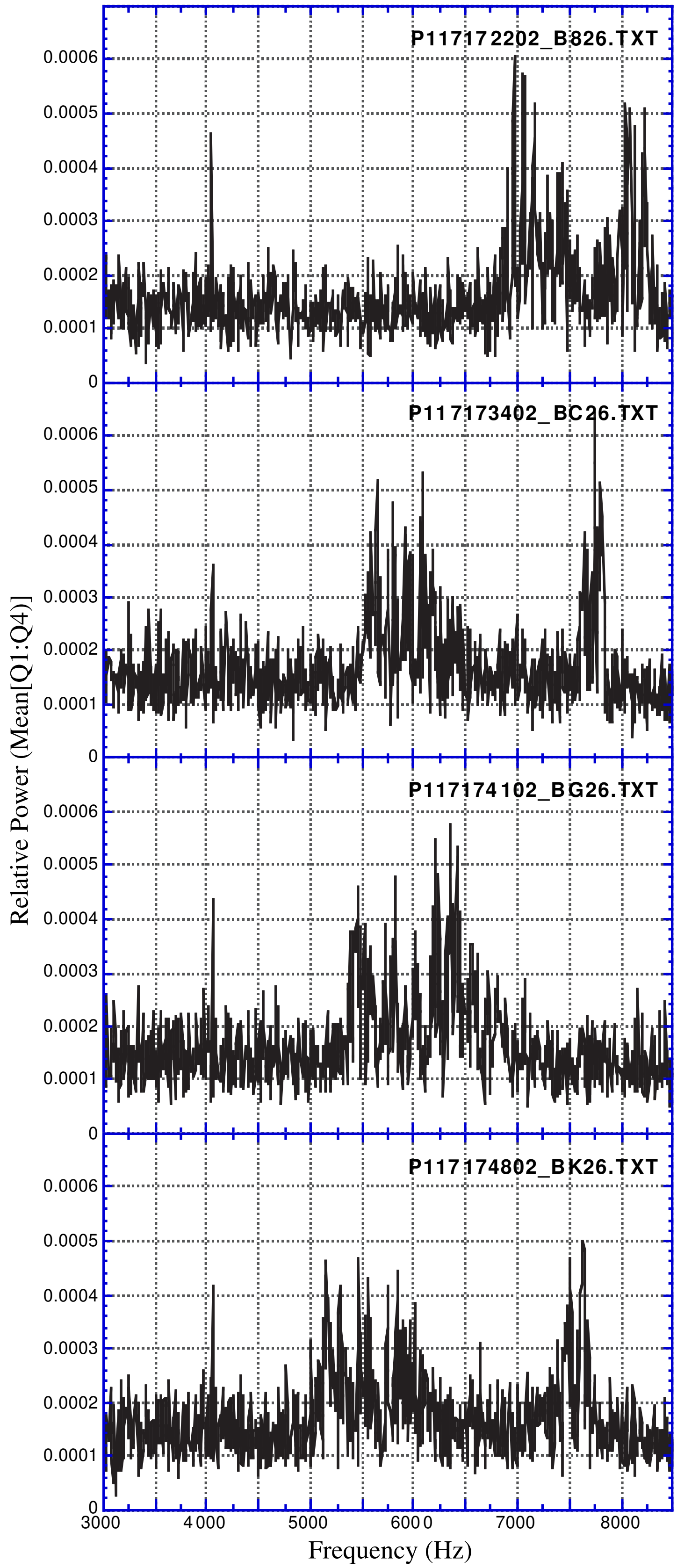

Figure 5. Temporal Variability in NCS ON 5kHZ-9kHz Power Spectra

The question of import is, are the noise amplitudes over these frequency bands sufficiently high to degrade the NICMOS images? In the absence of an absolute stimulus to unambiguously calibrate the excess power, I have undertaken a relative calibration which I believe is valid. The approach was as follows:

a) The power spectra from the NCS ON reference dark-subtracted images are essentially 1/f except for features intrinsic to the NCS and the residual BRZ 60Hz noise. Except for the contribution due to the NCS, the integrated power over all frequencies is equal to that in the read+electronic noise data.

d) One can subtract a 1/f power spectra from the NCS ON power spectra and scale the integrated residual power to that under the 1/f spectra and the RMS noise amplitude found from the read+electronic noise data. In particular, the averaged power spectra from all 4 quads are fit to a function of the form: $Y = a + b[\log(X)]$, where X is the frequency component. The 1/f-noise fit is subtracted from the observed power spectrum. The integrated power under the residual curve in the spectral region of interest is computed and ratioed to the total integrated power under the observed curve.

Doing the above, one finds, typically, that the power in the NCS induced noise typically increases the systemic noise amplitude by ~1% of the observed RMS read noise+electronic noise. Noting this was 310e-, the NCS-induced noise would increase the systemic noise per read pair by ~3e-. In flight, the read noise is ~35e-, so this would represent an increase of ~ 9% in the true read+systematic noise (i.e., a broadening of the read noise histogram).

Is this significant? If this were purely random noise with a 1/f spectrum the answer in most cases would probably be no, though this is subjective, and certainly others may argue. For some science programs where beating the data to the noise floor is essential that last 9% cold be meaningful. This noise, however, is concentrated in a band which corresponds to a temporal duration of ~125 to 200 microseconds or 10 to 20 pixels in extent with contiguous spatial structure along the readout direction (half of that scale peak-to-peak). Given the level of the noise introduced by the BRZ it is not surprising that this is difficult to see visually in the test dark data. This may pose more of a problem in the lower noise in-flight system.

8. SUMMARY

Power spectral analyses of NICMOS images taken with a flight spare array and replica electronics with the NCS connected to the test dewar and running indicate the presence of frequency-specific noise in a band from ~ 5 kHz to 9Khz. This is at a level which would be detectable, and measurable, with the flight-system electronics in the NCS era. Quantifying this low-level effect in terms of it's impact on science programs which will try to reach the noise floor is difficult. None-the-less, it is suggested that an attempt be made to locate and eliminate the source of this noise component in the NCS.

9. FINAL COMMENTS

An effort was made to reduce these data and perform the above initial analysis on the bulk of the data products as rapidly as possible. No doubt this report may raise new questions and subsequent analyses may be required. The above analysis, and inferences drawn by the author, should be viewed as a rapid attempt to pick the low hanging fruit from this data set. Almost certainly, additional information may be gleaned from the test data.

10. ACKNOWLEDGMENTS

I would like to thank Pete Hubbard and Tony Ferro (Steward Observatory/UofA) for their assistance in setting up the hardware and software required to carry out this test. I would also like to acknowledge the contributions made by numerous GSFC personnel and support contractors without whose help our portion of this test could not have been conducted. I am also grateful to Vicki Balzano at STScI for generating the test SMSs in a very short time.